

Topological phase for entangled two-qubit states

Pérola Milman^{1,2,*} and Rémy Mosseri^{3,†}

¹*Laboratoire Kastler Brossel, Département de Physique de l'École Normale Supérieure,
24 rue Lhomond, F-75231 Paris Cedex 05, France*

²*Collège de France, 11 place Marcelin-Berthelot, F-75005 Paris, France*

³*Groupe de Physique des Solides, Universités Pierre et Marie Curie Paris 6 et Denis Diderot Paris 7
2, Place Jussieu, 75251, Paris Cedex 05, France*

(Dated: October 29, 2018)

We present an unambiguous characterization of the rotation group $SO(3)$ biconnectedness topology using two-qubit maximally entangled states. We show how to generate cyclic evolutions of these states, which are in one-to-one correspondence to closed paths in $SO(3)$. The difference between the well known two classes of such paths translates into the gain of a global phase of π for one class and no phase change for the other. We propose a simple quantum optics interference experiment to demonstrate this topological phase shift.

PACS numbers: 03.65.Vf, 07.60.Ly, 42.50.Dv

Two-qubit states are the simplest quantum mechanical systems displaying entanglement. Maximally entangled states (MES) allow for a clear and measurable distinction between classical and quantum mechanical predictions, as exemplified by Bell type inequalities [1]. They also play a decisive role in quantum information processes, like teleportation or dense coding [2]. In addition, it is known that any quantum computing protocol involving many qubits can be implemented by concatenation of one or two-qubit gates [2]. This is why much attention has been paid to two-qubit systems, their properties and characterizations.

In the present work, we intend to show that two-qubit MES can also be used to display, even experimentally, the well known double-connectedness of the $SO(3)$ rotation group. Since the latter is often evoked to explain the minus sign multiplying a spin 1/2 state after a 2π rotation, we shall first argue that this is to some respect an ambiguous statement. Indeed, take one qubit state $|\Psi(t=0)\rangle = \alpha|0\rangle + \beta|1\rangle$ subject to the Hamiltonian $\hat{H} = \frac{\hbar\omega}{2}\hat{\sigma}_z$ (an effective magnetic field along the z axis). At time t , the state reads $|\Psi(t)\rangle = e^{-\frac{i\omega t}{2}}\alpha|0\rangle + e^{\frac{i\omega t}{2}}\beta|1\rangle$. Let us turn to the Bloch sphere representation of $|\Psi(t)\rangle$. The three coordinates are given by the expectation values of the Pauli matrices. As is well known, the expectation value of the spin precesses around the effective magnetic field. At $t = 2\pi/\omega$ it has experienced a full 2π rotation, and a π phase for the wave function. The π phase has been clearly demonstrated on several systems, starting with beautiful experiment on spin 1/2 neutrons [3]. On general grounds, the change of global phase γ under a cycle decomposes into its dynamical part, γ_d (as derived from the time dependent Schrödinger equation) and its geometrical part, the Berry phase γ_g , whose origin relies on the Hilbert space peculiar geometry. The latter phase, γ_g , equals half of the area bounded by the representing part of the Bloch sphere [4]. The dynamical phase γ_d is simply related to the time average of the Hamiltonian.

In the above case of one qubit precessing in a magnetic field, we have $\gamma_d = -\pi \cos \theta$ and $\gamma_g = -\pi(1 - \cos \theta)$, so the expected global phase $\gamma = \gamma_d + \gamma_g = -\pi$ for an initial state with $|\alpha| = \cos \theta/2$ and $|\beta| = \sin \theta/2$. Let us remark here that this π phase is present even for $\theta = 0$, where it is of pure dynamical nature (with no precession and therefore no rotation at all). We may therefore question the geometrical interpretation of the π phase. It would be more correct to state that this phase has a geometrical and a dynamical component, being purely geometrical only when $\theta = \pi/2$, when the initial state is orthogonal to the magnetic field. However, even in that case, we find problems in relating the phase to the double connectedness of $SO(3)$. Indeed, the latter property relates paths on the $SO(3)$ manifold, stating that, under continuous deformations there are only two different classes of paths, forming a two-element Z_2 first homotopy group: $\Pi_1(SO(3))$. Note that two dimensional rotations ($SO(2)$), have a more complicated structure: $\Pi_1(SO(2)) = Z$ [5]. The above experiment on a spin 1/2 particle was done with a constant magnetic field and therefore a constant rotation axis. A natural question is the relation of the measured π phase to topological properties of the rotation group: is the π phase related to the subtle nature of $SO(3)$ or to a property shared by $SO(3)$ and its subgroup $SO(2)$, as it seems to be the case? In the latter case, this phase gain is therefore not directly related to the $SO(3)$ double connectedness, but rather to a multi connectedness property shared by both groups.

In the following we aim to develop a non ambiguous relation between the $SO(3)$ topology and the global phase of a wave function. The idea is rather simple: we use the one-to-one map between $SO(3)$ and the set of two qubit MES [6]. A suitable set of Hamiltonians that keep constant the degree of entanglement is constructed, so that the two-qubit MES traces a path in $SO(3)$ when the orientation of the Hamiltonians is changed. The evolution is such that the dynamical phase vanishes while its ge-

ometrical counterpart, in a sense that will be precised, also vanishes, except at points where it abruptly changes to π . Note that such a π phase, although not related to the $SO(3)$ topology, has already been discussed in the context of entangled states [7].

A pure general bipartite state can be written as

$$|\Psi\rangle = \alpha|00\rangle + \beta|01\rangle + \gamma|10\rangle + \delta|11\rangle, \quad (1)$$

where α , β , γ and δ are complex coefficients satisfying the normalization condition. The complex concurrence \mathcal{C} of this state is defined as $\mathcal{C} = 2(\alpha\delta - \beta\gamma)$ and its norm equals the standard concurrence C for pure 2-qubits as defined by Wootters [8]. The concurrence C is a measure of the degree of entanglement for pure bipartite states, assuming the value $C = 1$ for maximally entangled states and $C = 0$ for product states. For the case of MES, state (1) can always be written (up to a global phase) in the general form [6]:

$$|\Psi\rangle = \sqrt{\frac{1}{2}}(\alpha|00\rangle + \beta|01\rangle - \beta^*|10\rangle + \alpha^*|11\rangle), \quad (2)$$

where the star denotes complex conjugation. The Hilbert space of all the MES can thus be defined as $\Omega_{MES} = \{(\alpha, \beta) \in C^2 / |\alpha|^2 + |\beta|^2 = 1, \text{ and } (\alpha, \beta) \sim (-\alpha, -\beta)\} = S^3/Z_2 = SO(3)$, i.e., there is an one-to-one correspondence between $SO(3)$ and the MES. This represents a sphere (in 4 d) whose opposite points are identified. By writing states in the form of Eq. (2), we can see that each MES can be denoted by a pair of complex numbers (α, β) .

We will now study closed trajectories in $SO(3)$, corresponding to the time evolution of MES subjected to precise Hamiltonians. The net result is that, depending on the homotopy classes to which the path belongs, the MES will acquire either a 0 or π phase. In the following we will show how this purely topological characteristics can be theoretically implemented and illustrated via an interference experiment.

Let's take as the initial MES the Bell state ($\alpha = 1, \beta = 0$)

$$|\Psi\rangle = \sqrt{\frac{1}{2}}(|00\rangle + |11\rangle). \quad (3)$$

In order to implement the cyclic evolution of state (3), we will consider simple polygonal trajectories in $SO(3)$: A sequence of evolution operators will act for a fixed finite time interval on the states, until they reach back the initial state (3). A geometrical picture illustrating this time evolution can be given by the hypercube of 16 vertices (belonging to S^3) depicted in Fig. (1). To get a discretized approximation of $SO(3)$ ($= S^3/Z_2$) we must identify opposite vertices, leaving altogether 8 distinct points, from A to H in Fig. (1), and the edges connecting these points. They all correspond to MES. The bar over

the letters denote the opposite points. Point A is our initial state (3) and point \bar{A} is identified to $-A$. The first class of trajectories that will be studied starts at A and finishes at the same point, making a circuit in the polygon defined by points $A \rightarrow B \rightarrow F \rightarrow D \rightarrow A$ in Fig. (1). This class will be called from now on the *plus* class, since it is homotopic to the identity and does not imply in a global phase change of the initial state. An example of the other class of trajectory, the *minus* class, is given by the sequence of points $A \rightarrow B \rightarrow F \rightarrow \bar{E} \rightarrow \bar{A}$. It also starts at point A but ends at the point diametrically opposed to the initial one (\bar{A}). Thus, there is a global phase of π gained by the initial state. Physically, this phase depends on the parity of the number of times the state crosses the space orthogonal to the initial one.

In order to keep the one-to-one relation between entangled states and $SO(3)$ elements, we will consider, in our trajectories, evolution operators leaving the complex concurrence \mathcal{C} constant. Taking $\hbar\omega = 1$, such unitary evolutions can be realized by the Hamiltonian $\hat{H} = \frac{1}{2}\vec{n}\cdot\vec{\sigma}$, which $\vec{\sigma} = \hat{\sigma}_x\vec{x} + \hat{\sigma}_y\vec{y} + \hat{\sigma}_z\vec{z}$, $\hat{\sigma}_x, \hat{\sigma}_y$ and $\hat{\sigma}_z$ and $\vec{n} = n_x\vec{x} + n_y\vec{y} + n_z\vec{z}$ is a normalized vector giving the orientation of the effective magnetic field. This Hamiltonian represents a rotation acting on only one of the qubits. The evolution operator corresponding to this Hamiltonian has the form:

$$\hat{U} = e^{-i\hat{H}t} = \begin{pmatrix} \cos \frac{t}{2} - in_z \sin \frac{t}{2} & -in_- \sin \frac{t}{2} \\ -in_+ \sin \frac{t}{2} & \cos \frac{t}{2} + in_z \sin \frac{t}{2} \end{pmatrix}, \quad (4)$$

where $n_{\pm} = n_x \pm in_y$. Defining $\epsilon = e^{i\pi/4}/\sqrt{2}$, we have, for the points appearing in the hypercube of Fig. (1): $A \rightarrow (1, 0)$, $B \rightarrow (\epsilon, \epsilon)$, $C \rightarrow (\epsilon^*, \epsilon^*)$, $D \rightarrow (\epsilon, -\epsilon)$, $E \rightarrow (\epsilon^*, -\epsilon^*)$, $F \rightarrow (i, 0)$, $G \rightarrow (0, 1)$, $H \rightarrow (0, i)$. By changing the interaction time t and the direction of rotation of our two-level system, i.e., vector \vec{n} , we are able to reach, departing from point A , all points in $SO(3)$, representing all possible MES. Notice that all rotations are performed on *one particle only*. In order to find the exact Hamiltonians that produce each class of trajectory, we will chose, for reasons that will become clear in the following, to perform the first two rotations in the first qubit and the last two in the second qubit. Thus, the total operator acting on our states can be written in the form $\hat{U} \otimes Id$ for the first half of the trajectory and $Id \otimes \hat{U}$ for the second one. One can easily check that in both cases the dynamical phases vanish. As for the geometrical phase, it can also be defined for open paths, as proposed by Pancharatnam [4]. This phase also vanishes in the present case, except when the state crosses the space orthogonal to the initial state, where it abruptly changes by π .

The parameters in equation (4) can be easily found by comparing this matrix to the necessary rotations to implement each part of the circuits. By doing so, we find that each part of the trajectory takes a time $t = 2\pi/3$ and

the only difference in the Hamiltonians is in the direction to which \vec{n} points. These orientations (n_x, n_y, n_z) read:

$A \rightarrow B$	$\sqrt{1/3}(-1, -1, -1)$
$B \rightarrow F$	$\sqrt{1/3}(1, -1, -1)$
$F \rightarrow D$	$\sqrt{1/3}(-1, -1, 1)$
$D \rightarrow A$	$\sqrt{1/3}(-1, 1, 1)$
$F \rightarrow \bar{E}$	$\sqrt{1/3}(1, -1, -1)$
$\bar{E} \rightarrow \bar{A}$	$\sqrt{1/3}(1, 1, -1)$

For both classes of trajectories, the Hamiltonians coincide from A to F , from where the vector \vec{n} will take a different value for each class of trajectory.

We will now address the question of measuring such an effect in an interference experiment. In order to test the topological phase, one needs a setup enabling the interference of an entangled state after performing one of the trajectories above with a reference one. A simple way to do that consists of interfering entangled photon pairs, as depicted in Fig. (2). Polarization entangled photon pairs are currently produced with high fidelity and efficiency in non linear optical systems [9]. Such twin photons propagate in different space modes, which will be denoted as a and b . Using this notation, the MES state emerging from a non linear crystal is $|\Psi\rangle = \sqrt{1/2}(|H_a V_b\rangle + |V_a H_b\rangle)$. Photons in modes a and b are detected by detectors D_a and D_b , respectively. Before detection, photons in mode b enter a Mach-Zender interferometer (see Fig.(2)). In the first 50% – 50% beam splitter (BS 1), mode b is combined to mode c , which is in the vacuum state, $|0_c\rangle$. After that, the total state is:

$$|\Psi\rangle = \frac{1}{2}(|H_a V_b 0_c\rangle + i|H_a 0_b V_c\rangle + |V_a H_b 0_c\rangle + i|V_a 0_b H_c\rangle), \quad (5)$$

which is exactly what is needed to interfere two entangled states: BS 1 produced two pairs of polarization MES, each one of them entangled to one arm of the interferometer. An experiment producing the reference fringes consists in the introduction of a variable phase factor $e^{i\phi}$ in arm b of the interferometer. Thus, before entering the recombining BS (BS 2), the state of the system is, taking into account the dephasing, $|\Psi\rangle = \frac{1}{2}(e^{i\phi}|H_a V_b 0_c\rangle + i|H_a 0_b V_c\rangle + e^{i\phi}|V_a H_b 0_c\rangle + i|V_a 0_b H_c\rangle)$. The passage through BS 2 changes the state into

$$|\Psi\rangle = \frac{1}{2}((e^{i\phi} - 1)(|H_a V_b 0_c\rangle + i|V_a H_b 0_c\rangle) + i(e^{i\phi} + 1)(|H_a 0_b V_c\rangle + |V_a 0_b H_c\rangle)). \quad (6)$$

Coincidence detections in detector D_a and D_b produce a counting rate $P = 1/2|(1 - \cos\phi)|$. The trajectories one want to implement are realized by photons in modes a and c . The space of polarizations, described by the

Poincaré sphere, is equivalent to the Bloch sphere [10]. For polarizations, all rotations in the Poincaré sphere can be accomplished via wave plates properly orientated introducing a dephasing in one of the polarization axis. The most general rotation matrix can be produced by a sequence of three wave plates: the first one introducing a dephasing of ψ in the vertical polarization axis, followed by the second one which introduces a dephasing of δ and makes an angle θ with the vertical polarization. Finally, a third plate introducing a dephasing of $-\psi$ in the vertical polarization can be added. As a result, a rotation matrix is generated which has exactly the same form as (4) with the following correspondence: the parameter δ plays the role of time t , while for the components of vector \vec{n} we have $n_x = -\sin 2\theta \cos \psi$, $n_y = \sin 2\theta \sin \psi$ and $n_z = \cos 2\theta$. We can thus introduce a set of plates acting in mode a and performing the common part of the trajectories, i.e., from point A to F . The remaining of the plates are put in arm b of the interferometer and their orientation determines the topology of the trajectories. The total state, before reaching BS 2, is then $|\Psi\rangle = \frac{1}{2}(e^{i\phi}|H_a V_b 0_c\rangle + i(-1)^n|H_a 0_b V_c\rangle + e^{i\phi}|V_a H_b 0_c\rangle + i(-1)^n|V_a 0_b H_c\rangle)$. The value of n (odd or even), depends on the nature of the trajectory. After passing through BS 2, the whole state transforms into

$$|\Psi\rangle = \frac{1}{2}((e^{i\phi} - (-1)^n)(|H_a V_b 0_c\rangle + |V_a H_b 0_c\rangle) + i(e^{i\phi} + (-1)^n)(|H_a 0_b V_c\rangle + |V_a 0_b H_c\rangle)). \quad (7)$$

If we now make the same coincidence counts in detectors D_a and D_b , we obtain the fringes $P = 1/2|((-1)^n - \cos\phi)|$. If the trajectory is of the *minus* class, a dephasing of one half period will be seen in the interference pattern. However, if it is of the *plus* type, the fringes remain at the same place. The choice of splitting the action of the rotations between the first and second qubit was made to stress the interest of using entangled states in the experiment. Since physics shall not depend on the order the detections were made, if we suppose that a detection in D_a is made, the rest of the state can be seen as a statistical mixture of polarizations. This means that dealing with entangled polarization pairs or with a completely unpolarized beam would produce the same results in our experiment. However, the one-to-one map from photon states to $SO(3)$ elements is only valid for MES and it is only in that case that we can claim probing a topological property of the rotation group.

The gain of the π phase factor, as mentioned before, is related to the number of times the MES crosses the space of its orthogonal states. An interesting variation of the experiment could well illustrate a different situation: one could think of trajectories which are not necessarily cyclic but, having crossed this orthogonal states space, already correspond to a gain of the π phase. This would mean that the final states interfering in BS 2 will no longer be the same MES. As a consequence, there will be a decrease

in the fringe visibility, but the desired dephasing would still appear.

Another interesting point to address is the case of states whose entanglement is not maximal. It can be shown that in that case, the π phase also occur. However, the relation between non MES and the $SO(3)$ group is more complex [6], as well as the geometrical interpretation of their time evolution.

The authors thank M. Brune, J. M. Raimond and S. Haroche for patient listening and fruitful comments and P. H. Souto Ribeiro for discussion of the experimental aspects. Laboratoire Kastler Brossel, Université Pierre et Marie Curie and ENS, is associated with CNRS (UMR 8552).

* Electronic address: Perola.Milman@lkb.ens.fr

† Electronic address: mosseri@gps.jussieu.fr

- [1] J. S. Bell, *Physics* **1**, 195 (1964); J. F. Clauser, M. A. Horne, A. Shimony and R. A. Holt, *Phys. Rev. Lett.* **23**, 880 (1969). For experiments, see A. Aspect, P. Grangier and G. Roger, *Phys. Rev. Lett.* **47**, 460 (1981); G. Weihs, *et al.*, *Phys. Rev. Lett.* **81**, 5039 (1998).

- [2] M. A. Nielsen and I. L. Chuang, *Quantum Computation and Quantum Information*, Cambridge University Press, Cambridge (2000).
- [3] H. Rauch *et al.*, *Phys. Lett.* **54 A**, 425 (1975); S. A. Werner *et al.*, *Phys. Rev. Lett.* **35**, 1053 (1975).
- [4] S. Pancharatnam, *Proc. Indian Acad. Sci. A* **44**, 247 (1956); M. V. Berry, *Proc. R. Soc. London A* **392**, 45 (1984); Y. Aharonov and J. S. Anandan, *Phys. Rev. Lett.* **58**, 1593 (1987).
- [5] C. Nash and S. Sen, *Topology and Geometry for Physicists*, Academic Press (1983).
- [6] R. Mosseri and R. Dandoloff, *J. Phys. A: Math. Gen.* **34**, 10243 (2001).
- [7] E. Sjöqvist, *Phys. Rev. A*, **62**, 022109 (2000); M. Ericsson, *et al.*, [quant-ph/0206063](https://arxiv.org/abs/quant-ph/0206063) (2002).
- [8] W. K. Wootters, *Phys. Rev. Lett.* **80**, 2245 (1998).
- [9] For some examples, see K. Mattle, *et al.*, *Phys. Rev. Lett.* **76** 4656 (1996); D. Bouwmeester, *et al.*, *Nature* **390** 575 (1997); D. Bouwmeester, *et al.*, *Phys. Rev. Lett.* **82** 1345 (1999); M. França Santos, *et al.*, *Phys. Rev. A*, **64**, 023804 (2002).
- [10] See, for example, Christian Brosseau, *Fundamentals of Polarized Light, a Statistical Optics Approach*, John Wiley and Sons, Inc. (1998); J. J. Sakurai, *Modern Quantum Mechanics*, Addison-Wesley (1994).

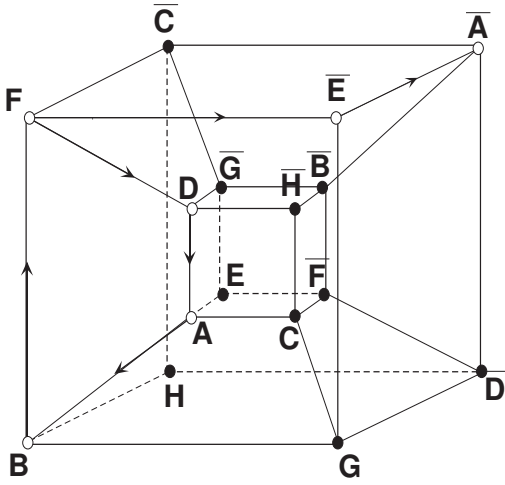


FIG. 1: Hypercube depicting the two topologically distinct trajectories. The *plus* circuit, corresponding to no phase change, is represented by the sequence of points $A \rightarrow B \rightarrow F \rightarrow D \rightarrow A$. The *minus* circuit, corresponding to the gain of a π phase, is the represented by the sequence $A \rightarrow B \rightarrow \bar{E} \rightarrow \bar{F} \rightarrow A$.

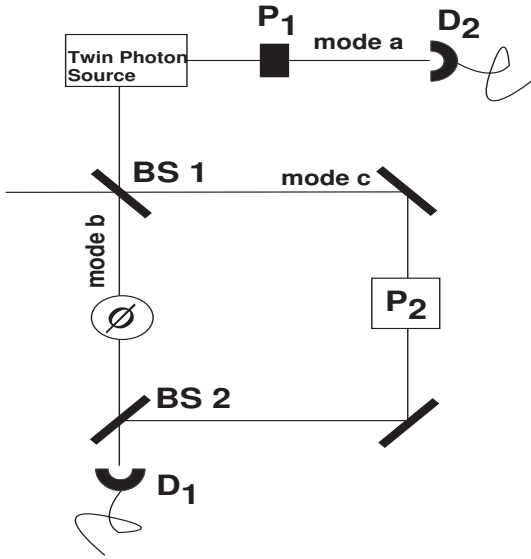


FIG. 2: Scheme for the experiment enabling the measurement of the global topological phase. Polarization MES are produced in the non linear crystal in modes a and b . Photons in mode b are combined to mode c in a Mach-Zender interferometer. A variable dephasing ϕ can be introduced in mode b , while wave plates properly oriented (P_1 and P_2) act on arms a and c , respectively, performing the desired trajectories